NUMERICAL SIMULATION OF CENTRIFUGAL PUMP OF LIQUID PROPELLANT ROCKET ENGINE

Marcel Vieira Duarte, marcelvduarte@gmail.com

Wladimyr Mattos da Costa Dourado, wladimyrwmcd@iae.cta.br

Instituto de Aeronáutica e Espaço, Praça Mal. Eduardo Gomes, 50, Vila das Acácias, 12228-904, Divisão de Propulsão Espacial, São José dos Campos, SP

Abstract. High-speed pumps, i.e., pumps with angular speed are widely used in aeronautics, missiles, naval, petrochemical industry and power plants. Because of high angular speed, they can be used without the application of gearboxes in Liquid Propellant Rocket Engines. The use of pumps of high rotational speed take into acount the requirements to get high pressures with small dimensions, reduced mass and few stages. The goal of this work is study the performance characteristics of a Liquid Oxygen pump applied to Liquid Propellant Rocket Engine. From the dimensions and the energy characteristics of the centrifugal pump, it is determined the performance parameters through the Computational Fluid Dynamics. From the numerical results generated by the simulation, improvements in the similar design are considered to optimize the efficiency of the pump through the analysis of the flow field inside the centrifugal pump. For volume mesh generation the software Gambit was used. To simulate the flow in centrifugal pump, the equations of Navier-Stokes with adequate boundary conditions are applied for three-dimensional geometry with the commercial software of finite volumes Fluent, assuming steady-state, incompressible flow conditions and without free gas dissolved in liquid. The model $\kappa - \epsilon$ is used to simulate the turbulent flow. Based in the results obtained, flow field and pressure distribution for different flow rates were analyzed. The characteristics curves of head, power and efficiency of centrifugal pump was ploted. The flow presented high instability due to probably presence of rotating stall in blades channels, as strong secondary flow and internal recirculation at suction and discharge of impeller for low flow rates (part load regime), affecting considerably its operation.

Keywords: Computational Fluid Dynamics, Propulsion, Liquid Propellant Rocket Engine, Turbopump, Pumps

1. NOMENCLATURE

H	specific work	**Subscripts**	
$\dot{m}$	mass flow rate	1	inlet
N	power	2	outlet
$\dot{m}$	mass flow rate	p	design
$\dot{V}$	volumetric flow rate	bl	blade
p	static pressure	0	eye impeller
c	absolute velocity	**Greek Symbols**	
z	blade number	ρ	density
b	width	η	efficiency
D	diameter	κ	turbulence kinetic energy
n_s	specific speed	ϵ	turbulence dissipation rate
		β	relative angle
		ι	angle of attack

2. INTRODUCTION AND BACKGROUND

2.1 INTRODUCTION

Flow in turbomachines, especially in centrifugal, is generally the most complex found in fluid mechanics. They are characterized by its three-dimensional aspect, viscous, unsteady, multiphase, turbulent and possible dependant of the geometric dimensions and conditions of operation. For this reason, numerical simulation as Computational Fluid Dynamics (CFD) in turbomachines has been very attractive.

The turbomachine design methods based on unidimensional techniques have been used for years as a powerful tool in the engineering of these machines. Without appealing to the great computational resources or labour time of computation, these methods produce valuable estimates of the main machine characteristics for the industry. However, they are incapable to supply a detailed analysis of the structure of the internal flow, which is indispensable for the study of some fluid dynamics phenomena of losses as cavitation, noise generation etc. So, they constitute an essential starting point in a global boarding for the design of a turbomachine. Then, the preliminary results were used for a refined and detailed study.

Turbomachine, as turbopumps applied to the Liquid Propellant Rocket Engine (LPRE), are designed using empirical relations that are developed based on experiments. Thus, the design of turbopumps is a complex and long task that involves some objectives and restrictions, being this task, generally, carried out an iterative process (Ovsyannikov and Borovskiy (1973)).

The L75 is a Brazilian LPRE fed for turbopump, which uses kerosene and Liquid Oxygen (LOx) as propellant. Its main requirements is thrust of 75 kN in vacuum for use in the upper stage of a satellite launch vehicle. Table 1 presents the main characteristics of this engine Torres *et al.* (2009).

Table 1: Main characteristics.

|	
Vacuum thrust	75 kN
Propellants	Kerosene/LOx
Pressurization	Turbopump
Combustion Chamber Pressure	70 bar
Mass flow rate	23.3 kg/s
Mixture ratio O/F	2.16
Vacuum specific impulse	328 s

2.2 BACKGROUND

Shojaee and Boyaghchi (2007) carried out numerical and experimental studies with centrifugal pumps (impeller and volute) having used water and oils of different viscosities for different outlet blade angles. They concluded that when outlet blade angles increase, the centrifugal pump performance improves. They also concluded that for more viscous oils the losses of performance increase due to the friction losses in the walls of the shroud as well as in the channels of impeller.

Panaiotti *et al.* (2007) analyzed the three-dimensional flow in centrifugal pumps using CFD. From the data obtained from the simulation, they designed a new centrifugal pump increasing the efficiency and head. Their work also shows zones of low pressure where it would have the possibility of cavitation occurrence at leading edge of the blades of impeller, while in the original pump these zones of low pressure appear in all the extension of the leading edge.

Oyama and Liou (2002) developed an optimization method for pumps using genetic algorithm. The objective was the maximization of the head and minimization of power of LOx pump for the engines M-1 and RL-10. The results overcame the original design increasing the head as well as reducing in the consumed power about 1%.

2.3 OBJECTIVES

The aim of this study is to investigate the flow inside the LOx centrifugal pump applied to the turbopump of the Brazilian LPRE L75 using CFD (Fig. 1). The numerical results are compared with the theoretical valvues estimated on the preliminary design. From the results it is possible to obtain the characteristic curves (specific work, efficiency and power) of the centrifugal pump for different operation conditions. From these curves it is possible to determine the best efficiency point (BEP), which is the operation of the impeller, that is the point of higher hydraulical efficiency.
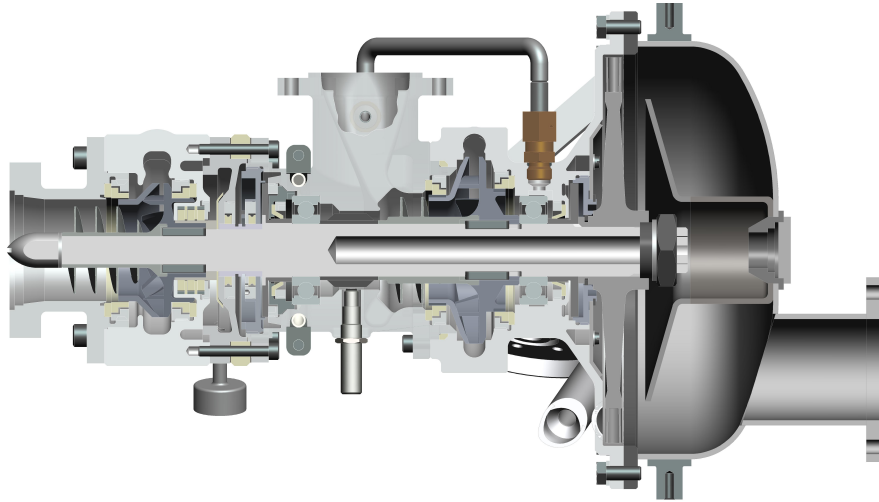
Figure 1: Illustration of L75 turbopump.

3. DESIGN OF LPRE PUMPS

Pumps and turbine are arranged in the so-called turbopump unit (TPU). The goal of TPU is supply to the LPRE of the necessary quantity of working components with required pressure created by the pumps, which are driven by a gas turbine.

The most common configuration in TPU is turbine, fuel and oxidizer pumps on the same axis supported by two bearings. When the turbine is positioned in the middle, the pumps are placed at the ends of the shaft. With LOx, the turbine in which operates at high temperature, is often placed at one end and to LOx pump at low temperature on the other end, with the fuel pump in the middle. This configuration simplifies the thermal analysis of the heat flow inside the casing and shaft of the turbopump.

For LOx pump at one end of turbopump, so-called cantilever pump, decreases inlet diameter and relative flow velocity at the blade input (Panaiotti *et al.* (2007)). It improves suction capability and decreases cavitation erosion.

The specific work of the pump H can be defined as, in kJ/kg:

$$H = \frac{p_2 - p_1}{\rho} + \frac{c_2^2 - c_1^2}{2} \tag{1}$$

where p_2 and p_1 are outlet and inlet static pressure, respectively; c_2 and c_1 are outlet and inlet velocity, respectively.

The hydraulic efficiency of the impeller (η) is defined as the ratio of the actual specific work and theoretical specific work:

$$\eta = \frac{H}{H_p} \tag{2}$$

The initial requirements for designing a high-speed LOx pump for turbopump applied to L75 LPRE are described in

Table 2.

Table 2

Description	Symbol	Value	Unity
mass flow rate	$\dot{m}$	15.97	kg/s
volumetric flow rate	$\dot{V}_p$	0.014	m³/s
temperature	T	90	K
inlet static pressure	p_1	0.35	MPa
outlet static pressure	p_2	9.42	MPa

A typical pump for LPRE are an inlet feed, inducer, centrifugal impeller, volute and connical diffuser has been designed based on the methodology by Ovsyannikov and Borovskiy (Ovsyannikov and Borovskiy (1973)) for LPRE.

Geometric and operation characteristics of this centrifugal impeller are summarized in Table 3. An overview of the impeller is shown in Fig. 2.

Table 3: Main dimensions of the impeller (Duarte (2011)).

Description	Symbol	Value	Unity
Blade number	z	8	-
External diameter	D_2	69	mm
Eye diameter	D_o	41	mm
Inlet diameter	D_1	39	mm
Inlet impeller width	b_1	12	mm
Outlet impeller width	b_2	7	mm
Inlet flow angle	β_1	9,7	°
Angle of attack	ι	13,5	°
Inlet blade angle	β_{1bl}	23	°
Outlet blade angle	β_{2bl}	41,3	°
Rotational speed	n	32468	rpm
Specific speed	n_s	91	-

4. METHODOLOGY OF NUMERICAL SIMULATION

First, the pump is modeled and three-dimensional fluid model is constructed by the software CAD SolidWorks. Then the model is exported to the software Gambit v2.4.6 where the computational mesh is generated. After that, it is exported to the commercial CFD software Fluent v6.3.26, where the processing and post-processing of the results is perfomed.

The turbulence model $\kappa - \epsilon$ is used to handle the turbulence of the flow due to its simplicity and robustness. These simulations are carried out for incompressible, steady-state flow, without presence of dissolved gases (single-phase flow) and used the technique of Multi-Reference Frame (MRF) to simulate the interaction between stationary and rotating parts.

The distributions of static, dynamic and total pressure on the surfaces of the impeller are studied. The behavior of the flow field in the interior is visualized for one better understanding of the phenomena as secondary flow, recirculation, etc.

4.1 MODELED DOMAIN

In the modeling of turbomachinery through CFD, it is necessary to solve some distance upstream and downstream of the blade passage (extent of domain). The boundaries should be placed far enough the blade order to ensure numerical stability and to minimize boundary condition effects (Younsi (2007)). The extent of domain also gives space to capture secondary flows and recirculations (especially in off-design operation cases). The computational domain obtained is shown in Fig. 3.
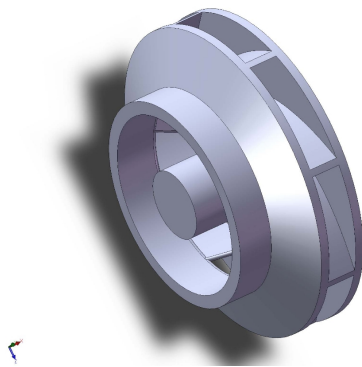
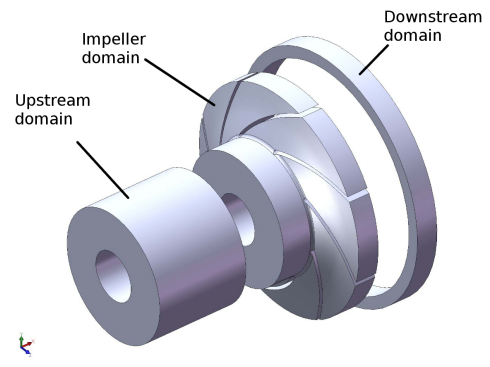**Figure 2:** Geometric model of impeller.

Figure 3: Computational domains.

4.2 MESH GENERATION

The modeled domain is composed of three domains: upstream, impeller and downstream domains. Table 4 summarizes the main characteristics of the grid for each fluid domain.

Table 4: Grid characteristics.

Fluid domain	Element	Number of cells	Nodes
Upstream	Hexahedral	192000	250082
Impeller	Prismatic/ Tetrahedral	1585115	410576
Downstream	Hexahedral	49920	56420
		Total	1827053

A structured hexahedral mesh was constructed in both upstream and downstream domains. For impeller domain, a boundary layer prismatic elements was defined on the blades walls, mainly next to the leading edge and trailing edge. So, it was create a eight layers, hence first layer thickness of 0.05mm and growth factor of 1.05, total thickness of 0.477mm. The final grid comprises 1827053 elements and can be seen in Fig. 4.
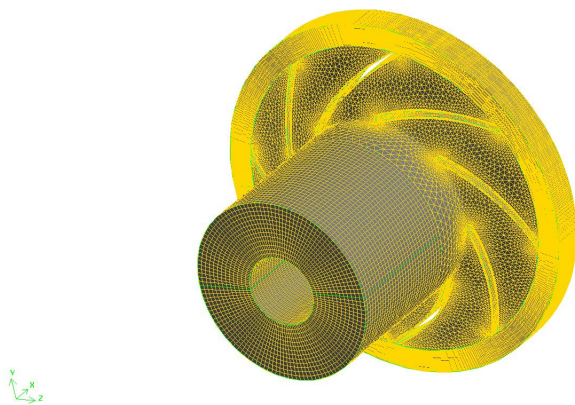
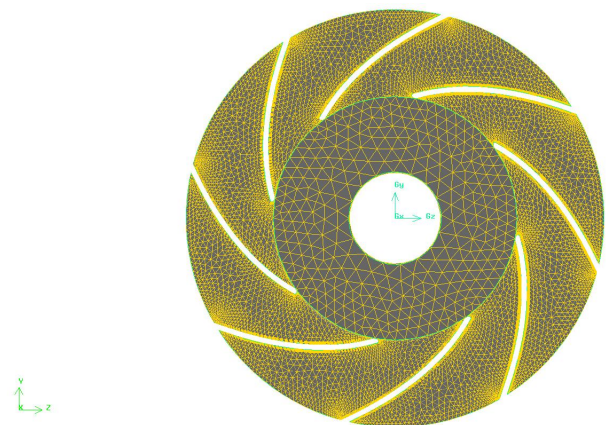

Figure 4: Computational mesh of impeller.

Figure 5: Computational mesh of impeller.

4.3 TURBULENCE MODEL

In this work, a commercial CFD code Fluent was used to study three-dimensional turbulent flow through the centrifugal impeller during design and off-design condition.

The $\kappa - \epsilon$ model was chosen as turbulence model due to its simplicity and robustness. The Standard $\kappa - \epsilon$ model is a semi-empirical model where the equations are determined based on empirical and phenomenological considerations.

The velocity scale (u_t) is defined by $u_t = \sqrt{\kappa}$. In the Standard $\kappa - \epsilon$ two-equation model is assumed that the length scale (l_t) is as dissipation length scale, and when the turbulence dissipation scales are isotropic, Kolmogorov (Wilcox (1998)) describes that:

$$\epsilon = \frac{\kappa^{3/2}}{l_t} \tag{3}$$

The effective viscosity is the sum of the flow viscosity and turbulent eddy viscosity $\mu = \mu_f + \mu_t$ where the turbulent viscosity is defined using the analogy of Prandtl-Kolmogorov:

$$\mu_t = \rho C_\mu \frac{\kappa^2}{\epsilon} \tag{4}$$

The turbulence kinetic energy (κ) and turbulence dissipation rate (ϵ) are obtained from the differentials transport equations, respectively:

$$\frac{\partial}{\partial t}(\rho\epsilon) + \frac{\partial}{\partial x_i}(\rho\epsilon u_i) = \frac{\partial}{\partial x_j}\left[\left(\mu + \frac{\mu_t}{Pr_\epsilon}\right)\frac{\partial \epsilon}{\partial x_j}\right] + C_{1\epsilon}\frac{\epsilon}{\kappa}G_\kappa - C_{2\epsilon}\rho\frac{\epsilon^2}{\kappa} \tag{5}$$

and

$$\frac{\partial}{\partial t}(\rho\kappa) + \frac{\partial}{\partial x_i}(\rho\kappa u_i) = \frac{\partial}{\partial x_j}\left[\left(\mu + \frac{\mu_t}{Pr_\kappa}\right)\frac{\partial \kappa}{\partial x_j}\right] - G_\kappa - \rho\epsilon \tag{6}$$

where G_κ represents the turbulent kinetic energy due to the velocities gradient given by:

$$G_\kappa = -\rho\overline{u_i' u_j'}\frac{\partial u_j}{\partial x_i}$$

where the values of the constants are obtained experimentally given by:

$$C_{1\epsilon} = 1.44; \; C_{2\epsilon} = 1.92; \; C_\mu = 0.09; \; Pr_\kappa = 1; \; Pr_\epsilon = 1.3.$$

4.4 NUMERICAL APPROACHES FOR TURBOMACHINERY

The commercial CFD code Fluent treats the problem of flows in moving reference frames, as in turbomachinery, with four numerical approaches: rotating rotor frame, multi-reference frame, mixing plane and sliding mesh. Multi-reference frame (MRF) is the most useful model for turbomachinery simulations. For transient stator-rotor interaction, sliding mesh provides better results than others approaches.

MRF commonly called frozen-rotor assumes that the flow is steady relative to the rotating frame, which simplifies the analysis. This model is suitable for flows having low interactions between the stator-rotor parts. The frozen-rotor approach gives results global average at each instant. The calculation results of steady values.

This model can be used as initial condition for transient calculations. The advantage of this approach is the computational time cost.

When the governing equations are solved in a reference rotational acceleration fluid particles, and other terms that appear in the equation of the quantity movement. The relative velocity is expressed in terms of absolute velocity by the expression as follows:

$$\vec{v}_r = \vec{v} - (\vec{\omega} \times \vec{r}) \tag{7}$$

where $\vec{\omega}$ is the angular velocity and $\vec{r}$ is the vector position of rotating reference.

The right term of the equation of momentum written in the formulation of absolute velocity:

$$\frac{\partial}{\partial t}(\rho \vec{v}) + \nabla \cdot (\rho \vec{v} \vec{v}) \tag{8}$$

In relative movement:

$$\frac{\partial}{\partial t}(\rho \vec{v}) + \nabla \cdot (\rho \vec{v}_r \vec{v}_r) + \rho(\vec{\omega} \mathbf{\ x\ } \vec{v}) \tag{9}$$

This expression can be described in the formulation of relative velocity:

$$\frac{\partial}{\partial t}(\rho \vec{v}_r) + \nabla \cdot (\rho \vec{v}_r \vec{v}_r) + \rho(2\vec{\omega} \mathbf{\ x\ } \vec{v}_r + \vec{\omega} \mathbf{\ x\ } \vec{\omega} \mathbf{\ x\ } \vec{r}) + \rho\frac{\partial \vec{\omega}}{\partial t} \mathbf{\ x\ } \vec{r} \tag{10}$$

where $\rho(2\vec{\omega} \mathbf{\ x\ } \vec{v}_r)$ represent the Coriolis term.

Finally, the momentum equations can be written in rotating coordinate system as follows:

$$\frac{\partial \rho}{\partial t} + \nabla \cdot (\rho \vec{v}_r) = S_m \tag{11}$$

4.5 BOUNDARY CONDITIONS

The equations describing the fluid flow through a specific domain need to be numerically closed stipulating the so-called boundary conditions. In this work the boundary conditions were specified as follows:

- Inlet: Total pressure and total temperature at inlet were considered.
- Oultlet: At the outlet the static pressure was specified. The outlet static pressure changes, obtaining the corresponding mass flow rate.
- Walls: all the surfaces of impeller were set relative velocity as zero. For upstream and downstream domain are set as zero.

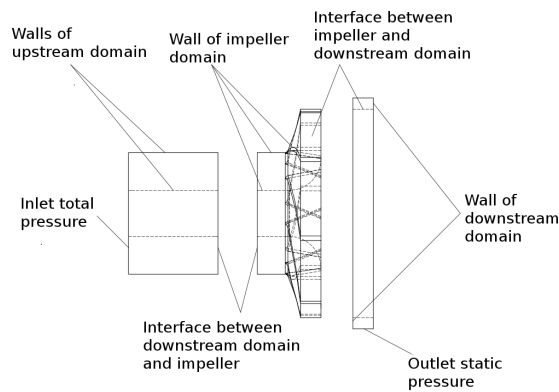Figure 6 depicts the boundary conditions adopted in the present work.

Figure 6: Boundary conditions.

## 4.6 NUMERICAL SCHEME TO SOLVE THE GOVERNING EQUATIONS

In the calculation of 3D flow field inside a centrifugal pump, the finite volume method is applied to transform the steady incompressible 3D Navier-Stokes equations into discrete ones. Then, Standard $\kappa - \epsilon$ model is adapted to turbulence calculation. Besides, SIMPLE algorithm (ANSYS (2006)) is used to solve pressure speed coupling equation group. The 2nd upwind scheme was used to calculate convective flux on the boundary surfaces of control volumes. This 2nd order

scheme is the least sensitive to mesh structure imperfections.

5. RESULTS AND DISCUSSION

The numerical results for ten operations points of the LOx centrifugal pump at temperature 90 K. The power is directly related with the pressure and viscous moments on the surfaces of impeller (hub, blades, shroud). The sum of these moments in relation to axis of rotation is the torque. Multiplying with angular velocity the power is determined. The inlet pressure is fixed and outlet pressure changed, obtaining the related mass flow rate.

Figure 7 shows the characteristic curves of specific work (H), power (N) and hydraulic efficiency (η) for different flow rates obtained by the numerical simulation. These curves are obtained for steady-state, single-phase flow, constant density and rotation.
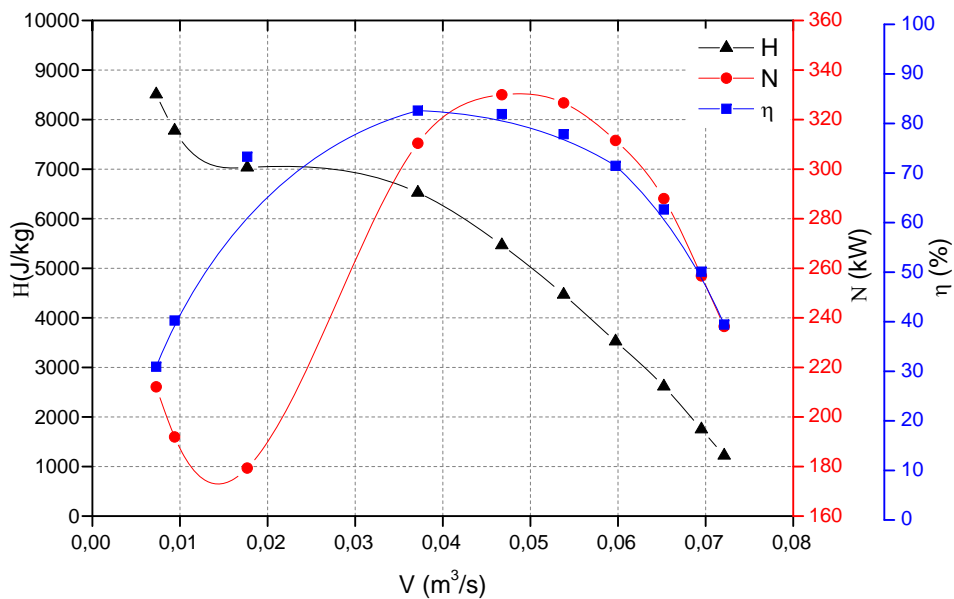
Figure 7: Characteristic curves of specific work (H), power (N) and hydraulic efficiency (η) of the impeller for constant rotation (32468rpm) and density (1140 kg/m^3).

From the numerical results, the hydraulic efficiency of the impeller in the preliminary design is equal to the obtained by CFD (83%), but for mass flow rate and specific work differents. These results for preliminary design of the centrifugal impeller and CFD results for the BEP ($\widetilde{V} = \dot{V}/\dot{V}_p 1$) are shown in Table 5.

Table 5: Comparison between the design and numerical conditions.

Parameter	Design	CFD
Specific work (J/kg)	8056	6526
Mass flow rate (kg/s)	15.97	42.36
Hydraulic efficiency of impeller	82.4	82.6

However, in the numerical simulations in part-load regime (volumetric flow rate below the BEP, $\widetilde{V} < 1$), the impeller has presented recirculation in the suction as well as discharge side, as well as the presence of secondary flow. These phenomena increase the hydraulic losses, affecting considerably the format of the characteristic curves of specific work, power and efficiency. Figure 8 shows the flow pathlines in BEP and Fig. 9 depicts the part load regime. Another phenomenon that affects the format of the characteristic curve was the probable presence of rotating stall.

The distributions of pressure and velocity for overload regime ($\widetilde{V} > 1$) showed a smooth and uniform flow field in the channels. The static pressure showed a higher contribution in the total pressure than the dynamic pressure.
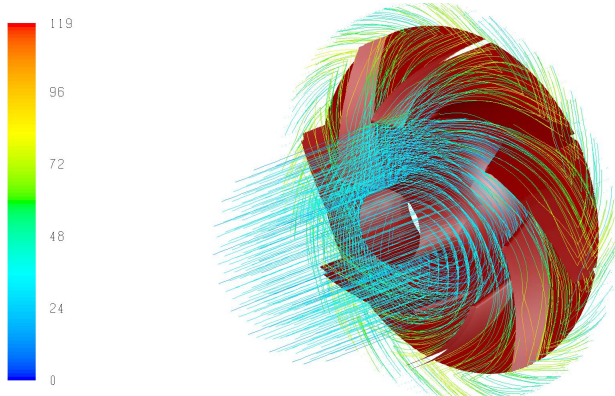
Figure 8: BEP for $\widetilde{V} = 1$.
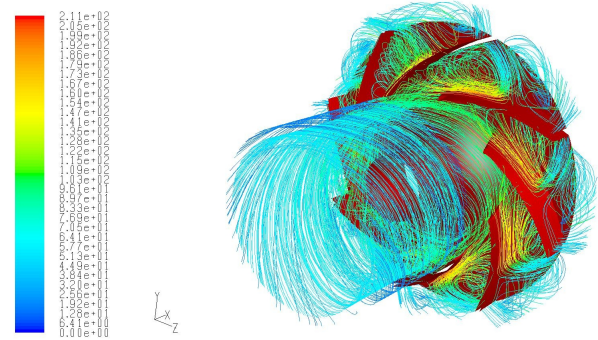
Figure 9: Partload regime for $\widetilde{V} = 0.48$.

For part-load regime ($\widetilde{V} < 1$) the numerical results showed a stronger non-uniformity in the distributions of pressure and velocity due to strong recirculation at the suction and discharge of the impeller, secondary flow, and flow separation at pressure side of blade, which can be characterize a possible presence of rotating stall, which contributes strongly in the viscous energy loss of the impeller. The generation of a more refined mesh could improve the visualization of secondary flow phenomena, flow separation and rotating stall between channels of impeller.

The distributions of pressure and velocity for overload regime ($\widetilde{V} > 1$) showed a smooth and uniform flow field in the channels. The static pressure showed a higher contribution in the total pressure than the dynamic pressure.

For part-load regime ($\widetilde{V} < 1$) the numerical results showed a stronger non-uniformity in the distributions of pressure and velocity. This flow pattern was due to strong recirculation at the suction and discharge of the impeller, secondary flow and flow separation at pressure side of blade, which can be characterize a possible presence of rotating stall, which contributes strongly in the viscous energy loss of the impeller. a more refined mesh could improve the resolution of secondary flow phenomena, flow separation and rotating stall between channels of impeller.

6. CONCLUDING REMARKS

For the numerical simulations SIMPLE algorithm is used to solve the equations that govern the steady flow, incompressible viscous inside the pump for different operating conditions. Despite its limitations, the turbulence model Standard $\kappa - \epsilon$ was adopted to describe the turbulent flow because of its robustness and low computational cost. The rotor-stator interface technique used to Multi-Reference Frame (MRF) was used because it provides satisfy results for turbomachinery at steady state. The boundary conditions are properly considered at inlet (total pressure), outlet (static pressure) and moving walls of the impeller and stationary walls of the upstream and downstream domains.

The numeric results for different conditions allowed determination of the characteristics curves for the centrifugal pump at constant rotational speed of 32458 rpm. About the characteristic curves obtained by numerical results, the efficiencies obtained in the hydraulic design of the impeller and are numerically equal (82.4% and 82.6%, respectively), the results obtained numerically for BEP of the impeller was for a mass flow of 43 kg/s if a specific work of 6526 J/kg, of different design requirements initials of 15.97 kg/s 8056 J/kg respectively.

The pump characteristic curve was obtained numerically, which showed strong instability for flows below the point of highest efficiency obtained numerically, due to the presence of strong recirculation discharge, secondary flow and probable presence of rotating stall.

For the BEP ($\widetilde{V} = 1$), impeller has been presented uniform pressure distribution and uniform flow field in the channel, without the presence of recirculating secondary flow, rotating stall or pre-rotating flow in the impeller inlet.

At off-design condition ($\widetilde{V} \neq 1$), mainly at for part-load regime ($\widetilde{V} < 1$), the flow pattern has showed stronger non-uniformity in the pressure distribution and velocity field. The main reason are due to strong recirculation at the suction and discharge of the impeller, secondary flow, flow separation at pressure side of blade, which strongly contributes to

losses of the centrifugal impeller.

Although recirculation phenomena is difficult to understand and one or more geometric parameter can not predict the suction or discharge recirculation into the pump. It can be proposed some suggestions to improve the design, such as reducing the eye impeller diameter and reducing the angle of attack of the blade (ι). Another possible solution would be the presence of a component of rotation in the impeller inlet. In the numerical simulation has been neglected the presence of inducer and the flow has been adopted flow normal to the inlet surface of the upstream domain. Another possible solution can be the numerical simulation interaction between pump and volute, analyzing its real influence in the discharge recirculation.

7. ACKNOWLEDGEMENTS

The authors would like to thank Agência Espacial Brasileira (AEB), Instituto de Aeronáutica e Espaço (IAE) and Instituto Tecnológico de Aeronáutica (ITA) for their valuable contributions to this project.

8. REFERENCES

ANSYS, 2006. *Ansys Fluent v6.3.26 User's Guide*. 2006.

Duarte, M.V., 2011. *Projeto e Análise por Mecânica dos Fluidos Computacionais de uma Bomba Centrífuga Aplicada a Motor Foguete a Propelente Líquido*. Master's thesis, Instituto Tecnológico de Aeronáutica.

Ovsyannikov, B.V. and Borovskiy, B.I., 1973. *Theory and calculation of feed units of liquid propellant rocket engines*. Ohio:Foreign Technology Division.

Oyama, A. and Liou, M., 2002. "Multiobjective optimization of rocket engine pumps using evolutionary algorithm". *Journal of Propulsion and Power*, Vol. 18, No. 3,, pp. 528–535.

Panaiotti, S.S., Rohatgi, U.S., Timushev, S.F., Soldatov, V.A. and Chumachenko, B.N., 2007. "CFD study of prospective 1st stage centrifugal impeller design". In *5th Joint ASME/JSME Fluids Engineering Conference, San Diego, California USA*. PANAIOTTI, S. S.; ROHATGI, U. S.; SOLDATOV, V. A.; CHUMACHENKO, B. N.;.

Shojaee, M.H. and Boyaghchi, F.A., 2007. "Studies of the influence of various blade outlet angles in a centrifugal pump when handling viscous fluids". *American Journal of Applied Sciences*, Vol. 9, pp. 718–724.

Torres, M.F.C., Almeida, D.S., Krishna, Y.S.R., Silva, L.A. and Shimote, W.K., 2009. "Propulsão líquida no iae: Visão das atividades e perspectivas futuras". *Journal of Aerospace Technology and Management*, Vol. 1, pp. 99–106.

Wilcox, D.C., 1998. *Turbulence modeling for CFD*. DCW Industries.

Younsi, M., 2007. *Aéroacoustique et aérodynamique instationnaire, numérique et experimentale des ventilateurs cen-trifuges action*. Ph.D. thesis, L'École Nationale Supérieure d'Arts et Métiers.